# Ultra-Fast Fluorescence Decay in Natural Carotenoids

*W. Becker, A. Bergmann, C. Junghans*
*Becker & Hickl GmbH, Berlin, Germany*

*Abstract:* We used the bh DCS-120 MP multiphoton system with fs-laser excitation and ultra-fast detectors to record the fluorescence decay of natural carotenoids. In all cases, the fluorescence was dominated by fast decay components, with lifetimes down to 8.6 ps and amplitudes up to 99%.

## Motivation

Carotenoids are present in almost any live species on this planet. In plants and algae, they assist photosynthesis via an additional light-harvesting complex and protect the cells against photo-oxidative stress [15]. In animals, carotenoids and their derivatives are providing the colours of fish, reptiles, and birds. Moreover, carotenoids play a role as UV absorbers and as scavengers of reactive oxygen species. In mammals, carotenoids are present in almost all organs, such as skin, liver, brain, ovaries, prostate, and blood [11, 13, 17]. In the eye, carotenoids present a dominating portion of the macular pigment [16].

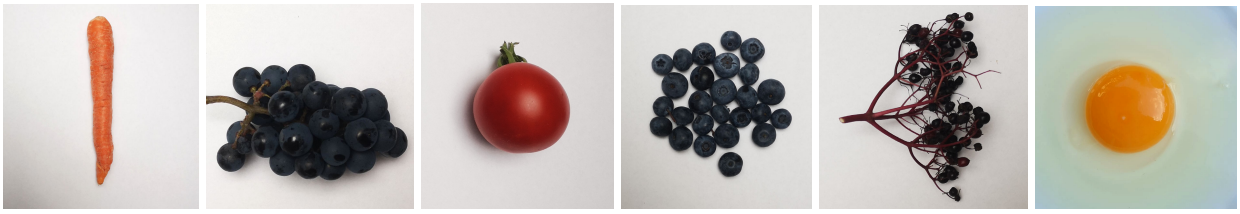

Fig. 1: Carotenoids from the objects shown were investigated in the study presented here. Left to right: Carrot, grape, tomato, blueberry, elder fruits, egg yolk.

It is presumed - in some cases even known - that carotenoids are essential to the function of the organs. Moreover, there are indications that they act as anti-oxidative and anti-inflammatory agents, and that they have anti-bacterial, anti-viral, and even anti-cancer functions [10]. Well known is the effect of β-carotene and lutein on the macula of the human eye [10, 16].

It would therefore be desirable to investigate these effects directly on the cell level. This can be done best by using fluorescence lifetime and fluorescence lifetime imaging (FLIM) techniques [1, 2]. For example, the metabolic state of a cell can be determined by FLIM of NADH and FAD [2]. With this technique, possible effects of physiologically active compounds can be seen within minutes, compared to weeks, months or even years required for clinical studies. In such studies, it would be desirable to see not only the effect on the cell metabolism but also the uptake and metabolisation of the carotenoids themselves. Unfortunately, there is a problem: Carotenoids are virtually non-fluorescent. Fluorescence quantum yields given in the literature are on the order of $10^{-4}$ to $10^{-5}$ [12] so that detection of fluorescence is extremely challenging. This is especially the case in a biological environment where other fluorophores with much higher quantum yield are present.

Fortunately, the problem of low fluorescence quantum efficiency is less relevant for time-resolved measurements. Low quantum efficiency means that the non-radiative decay rate is much higher than the radiative one. In turn, that means that the fluorescence decay time becomes short. It can become *very short*, if the quantum efficiency is on the order of $10^{-3}$ or less. In practice, there is a

reciprocal relation between the fluorescence lifetime, $\tau_{fl}$, and the fluorescence quantum efficiency, $QE_{fl}$ :

$$\tau_{fl} = \tau_0 / QE_{fl}$$

$\tau_0$ = natural fluorescence lifetime in absence of non-radiative decay

Importantly, the fluorescence quantum efficiency has no influence on the intrinsic peak intensity of the fluorescence decay function. Technically, that means that the fluorescence is well detectable as long as the lifetime remains longer than the temporal resolution, or the 'IRF' width [2]) of the measurement system. Please see Fig. 2.

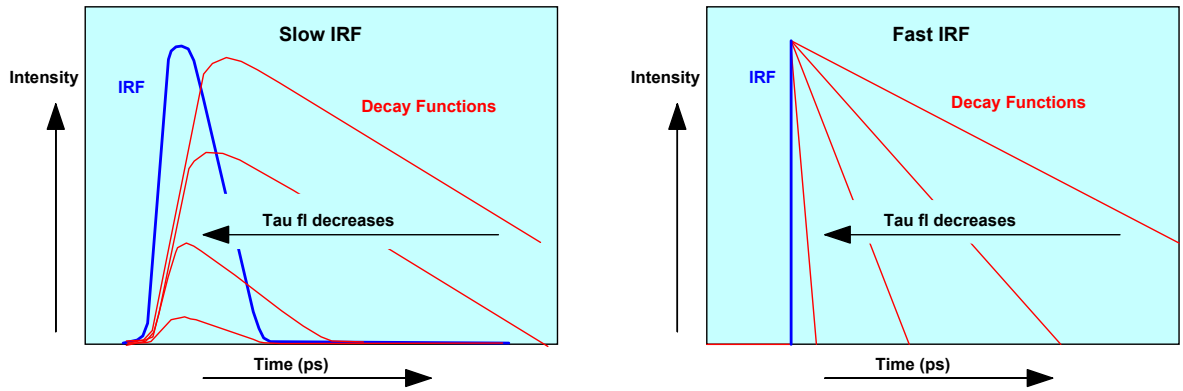


Fig. 2: Amplitude of recorded decay functions for different $\tau_{fl}$. Left: With a slow IRF the amplitude of the recorded curve decreases with decreasing lifetime. Right: With a fast IRF the amplitude remains constant.

## Experiment Setup

For the measurement of extremely fast fluorescence decay a short IRF of the excitation and detection system is essential. We therefore used our DCS-120 MP multiphoton FLIM system [6] for recording the data. Since the excitation pulses have femtosecond width the pulse shape does not contribute to the effective IRF of the system. Moreover, in contrast to cuvette systems, there is no geometric broadening of the IRF by transit-time differences in the cuvette and in a monochromator. In combination with ultra-fast hybrid detectors and ultra-fast TCSPC/FLIM modules the system delivers an IRF width of less than 20 ps, FWHM [5]. A photo of the DCS-120 MP is shown in Fig. 3, left, the optical principle is shown in Fig. 3, right.

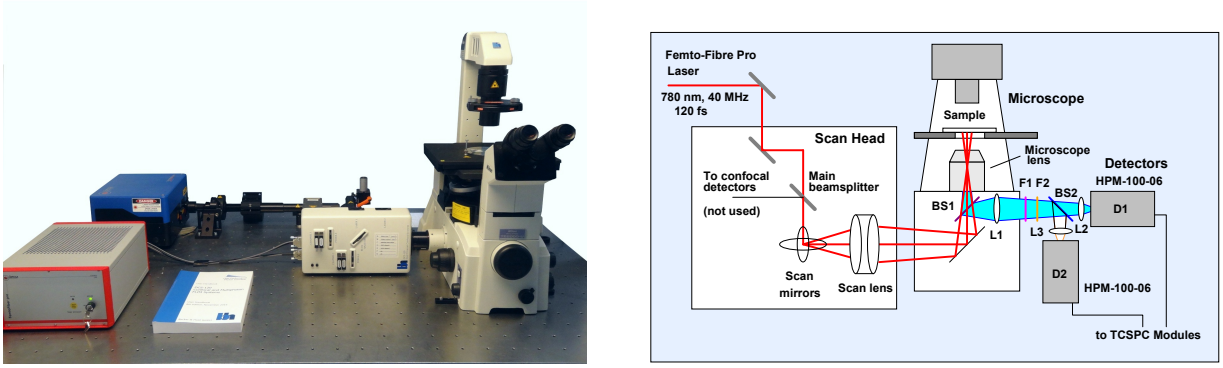


Fig. 3: Left: DCS-120 MP FLIM system. Right: Principle of optical system

The system consists of a Toptica Femto-Fibre Pro laser (780 nm, 40 MHz, 120 fs), a bh DCS-120 scan head [2, 6, 7], a Nikon TE 2000 inverted microscope, non-descanned detection optics, and bh

HPM-100-06 hybrid detectors [2, 5]. The single-photon pulses of the detectors are processed by two parallel SPC-180NX TCSPC / FLIM modules (electrical IRF width 3.5 ps) [2, 3]. For further details please see [2] and [6].

## Procedures

Extracts from the objects under investigation were obtained by gently heating them to about 60 °C and pressing fluid out of them. The extracts were placed in Ibidi cell dishes which were put under the microscope. The image plane was selected first visually by identifying the glass / solution interface, and then shifting the focus further into the solution by an estimated 10 µm. The correctness of focusing was checked in the 'Preview' mode of the DCS-120 system. Decay data were taken in the 'Single' mode of SPCM software while letting the system scan an area of about 50 µm. Scanning was used to avoid heat concentration in the detection volume. An NA=1.3 oil immersion objective lens was used. The high NA not only provides maximum excitation and detection efficiency, it also cancels possible anisotropy-decay effects [2]. The data were collected in Detector 1 only, with filters F1 = 680 nm short pass and L2 = 400 nm long pass (see Fig. 3). That means virtually all fluorescence from 400 nm to 680 nm was recorded. F1 bocks residual excitation light, F2 blocks possible second-harmonic generation (SHG) light from the detectors.

It may be objected that 780 nm is not the best excitation wavelength for carotenoids. One-photon absorption maxima are in the range of 450 to 500 nm [14], so that the two-photon absorption maximum should be expected around 900 to 1000 nm. However, 2-photon excitation spectra are usually broader than 1-photon spectra, and there is always some absorption at the short-wavelength side of the maximum. As a result, there were no problems to obtain reasonable intensities from all sample investigated. Typical count rates were 50,000 $s^{-1}$ to 100,000 $s^{-1}$, with a laser power of 5 to 10 mW in the sample plane.

## Results

### Carrot

The carrot is the prototype of carotene-containing plants in that the pigment is composed almost completely of β-Carotene. A decay curve of carrot extract is shown in Fig. 4.

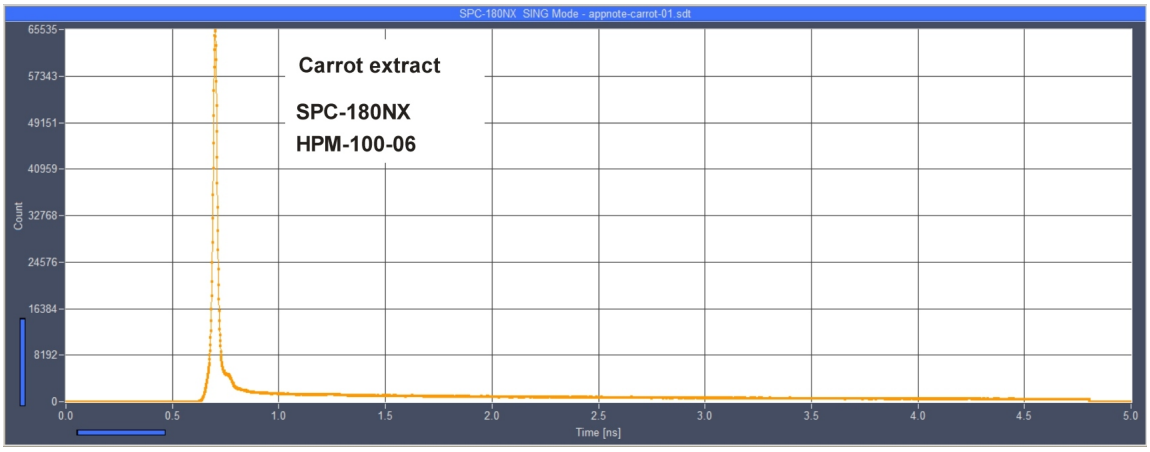


Fig. 4: Decay function of carrot extract. Linear scale, 1.2 ps / time channel, 4096 channels, total recording-time interval 5 ns.

As expected, the decay curve is dominated by an ultra-fast component. To give an impression of how strong the component is, the curve is shown in linear scale. Analysis with SPCImage NG yields a component lifetime of 8.6 ps, and an amplitude of 99 %, see section 'Analysis with SPCImage NG'.

To make sure that the recorded signal comes from β-carotene we recorded a decay curve from the purified compound. As can be seen from Fig. 5 the decay curves of the pure β-carotene and the carrot extract are virtually identical, confirming that the signal from the carrot is indeed β-carotene fluorescence.

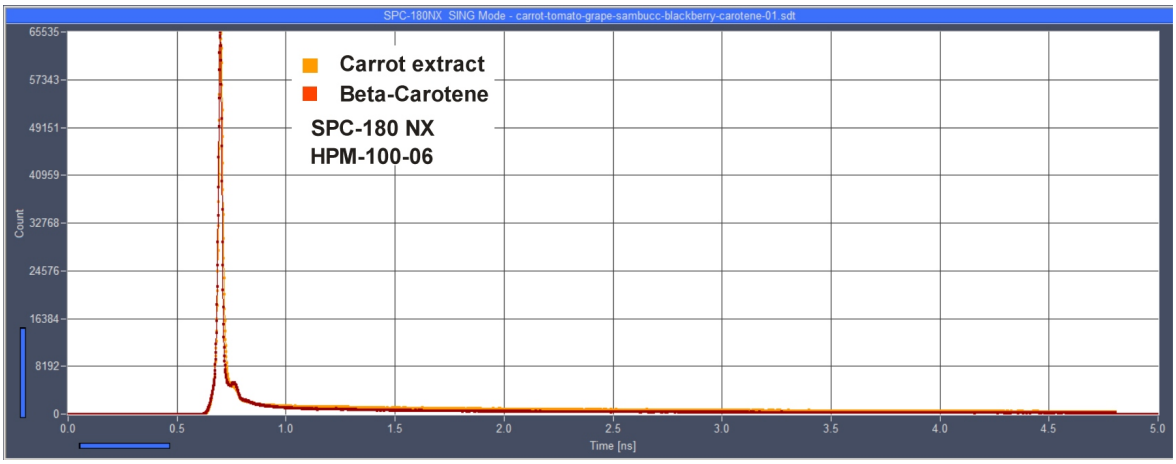


Fig. 5: Decay curves of carrot extract and purified β-Carotene. The decay functions are virtually identical.

## Where in the Carrot is the β-Carotene?

To find out where in the carrot cells the β-Carotene is located we performed 2-photon FLIM measurements of carrot tissue. In the FLIM images, the presence of β-carotene is conveniently visible in the amplitude-weighted lifetime, tm, of a triple-exponential decay analysis. In locations where β-carotene is present tm is shorter than 100 ps, in locations where it is absent tm is in the range of 3 ns. An example is shown in Fig. 6. The image shows that the β-carotene is not evenly distributed but concentrated in distinct clusters within the cells.

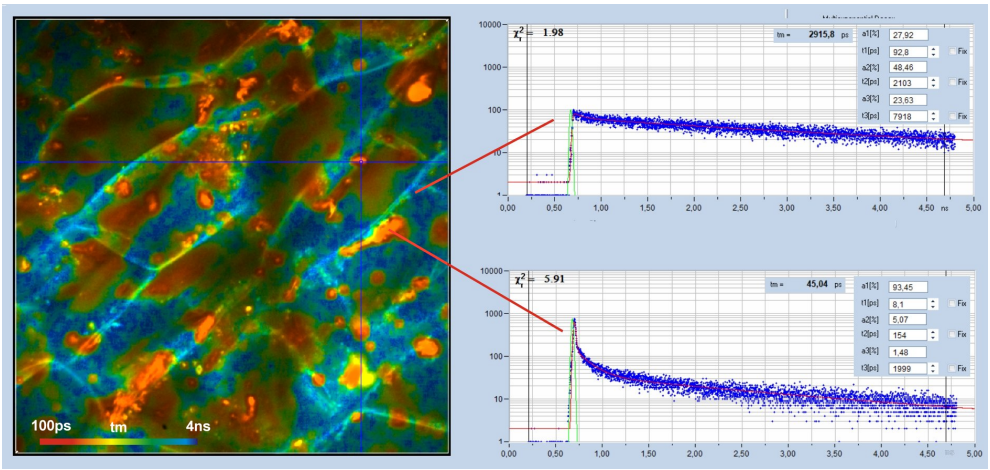


Fig. 6: Lifetime image of carrot tissue. Amplitude-weighted lifetime, tm, of triple-exponential fit. Decay curves in locations without and with β-carotene shown on the right.

## Other Plant Pigments

We recorded decay data from a number of pigmented fruits which are commonly found in urban environment. In all cases we found ultra-fast decay components of high amplitude. Fig. 7 shows decay curves of extracts of grape, tomato, blueberry, and black elder fruits. An interpretation of the data is difficult because fruits contain mixtures of different carotenoids. Moreover, carotenoids are not the only pigments in fruits. Also anthocyanins may be present or even dominant [11]. The presence of anthocyanins can be seen from the pH dependence of the colour which is characteristic of anthocyanins but not of carotenoids.

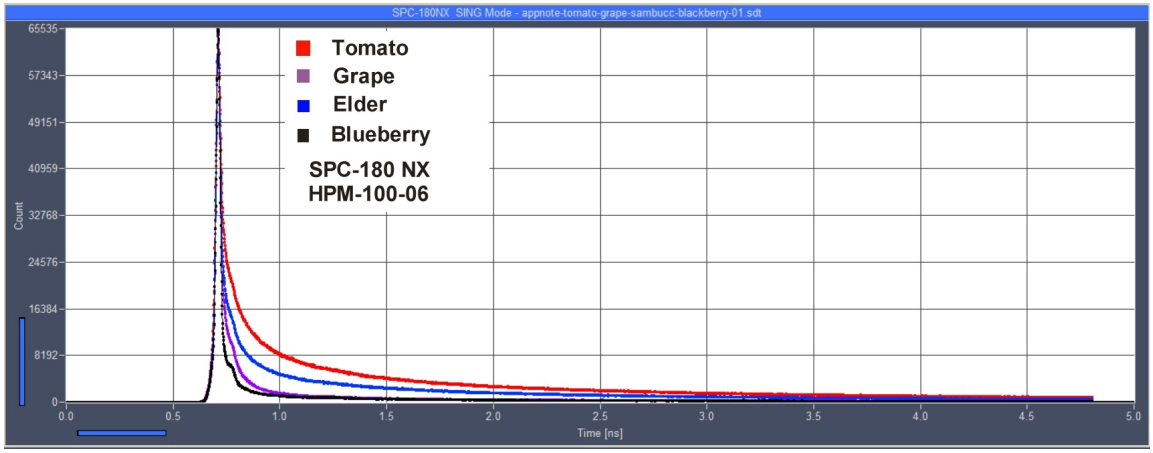


Fig. 7: Decay curves of extracts of tomato, grape, blueberry, and black elder.

For comparison, Fig. 8 shows decay curves of a number of pure carotenoids and anthocyanins. Not surprisingly, also the pure substances show extremely fast decay components.

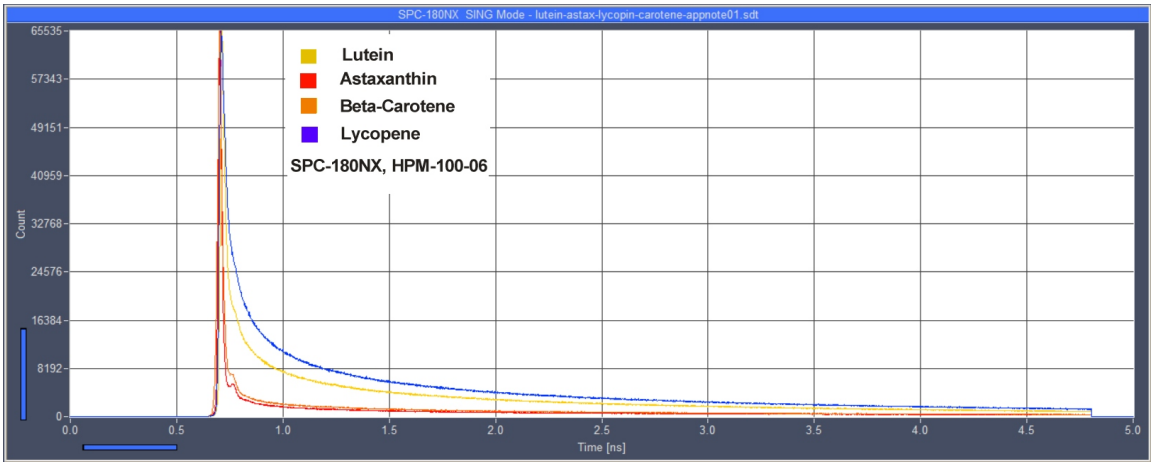


Fig. 8: Decay curves of lutein, astaxanthin, β-carotene, Lypcopene

## Egg Yolk

Egg yolk contains lutein and zeaxanthin. The compounds are very similar to β-carotene, differing only in the end groups of the conjugated double-bond chain. Lutein and zeaxanthin are isomers, differing in the location of one double bond in one of the end groups [13]. Because the length of the double-bond chain does not differ by much it can be expected that the spectroscopic properties are very similar. Fig. 9 shows decay curves of egg yolk and egg white. As expected, the decay curve of the yolk shows an ultra-fast component. However, there are also slower components. It is not

known whether these come from special modifications or special binding states of lutein or zeaxanthin. Another (and possibly more likely) explanation is that the components are fluorescence of NAD(P)H and/or FAD.

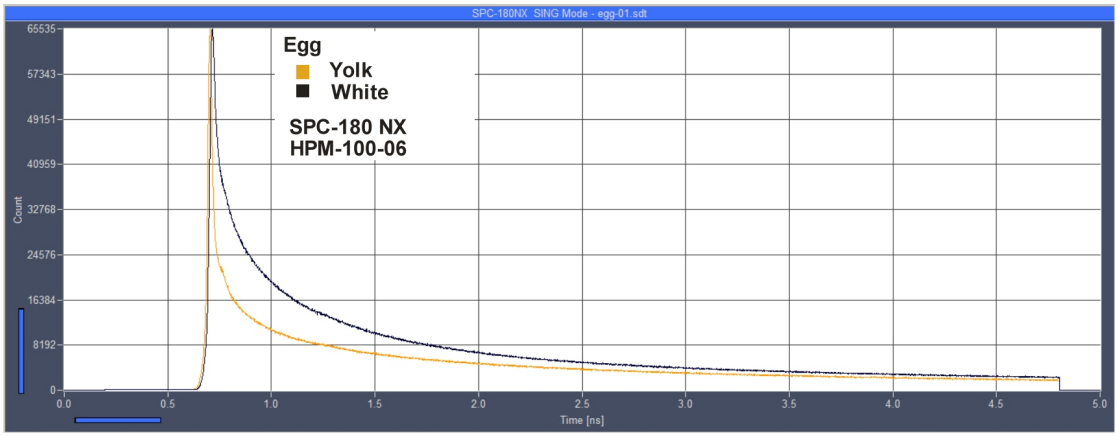


Fig. 9: Decay curves of egg yolk and egg white

For comparison, the figure also shows a decay curve of the white of the egg. The fluorescence intensity is about 100 times lower than in the yolk, the decay time of the fast component is 44 ps, and there is more background of slower fluorescence. The lifetimes of the slow components are 507 ps and 3.5 ns, compatible with the assumption that the slow fluorescence comes from NAD(P)H or FAD or a mixture of both. This would even be an explanation of the fast component of 44 ps. As has been shown in [8], FAD has a fast decay component of about 55 ps which could easily account for the fast component.

## Analysis with SPCImage NG

The lifetimes of the fast decay components are close to or shorter than the IRF width of the detector. In principle, the resolution could be increased by superconduction single-photon detectors (SSPDs, IRF width 4.4 ps FWHM, including TCSPC) [9] or, possibly, ultra-fast single-photon avalanche diodes (SPADs). However, such detectors have extremely small active areas so that their use in a laser-scanning microscope is not practicable.

It was therefore attempted to determine the lifetimes with SPCImage TCSPC/FLIM analysis software. In principle, SPCImage can determine lifetimes substantially shorter than the FWHM of the instrument response by de-convolution. This requires, however, that the IRF be exactly known. SPCImage provides two ways to include the IRF in the calculation. The first one is to use a synthetic IRF. The IRF is modelled by a function of the type $t \cdot e^{-t/t0}$, with the parameter t0 being determined by a fit procedure [2, 4]. The procedure is easy to use but does not account for possible bumps in the IRF. Low-amplitude bumps in the IRF do not change the result significantly but make it difficult the judge the quality of the fit.

The second way is to use a measured IRF. This accounts for possible irregularities in the IRF shape but requires accurate measurement of the IRF in exactly the same instrument configuration as used for the fluorescence measurement. For a sub-20-ps IRF this is not easy.

As can be seen in Fig. 4 and Fig. 5 the IRF of the detector is not entirely free of an afterpulse. For analysis of the data we therefore used a measured IRF. The IRF was recorded from the SHG of

finely powdered sugar. Care was taken to avoid optical reflections (SHG is emitted in forward direction!) and to avoid transit-time changes by different filter thickness.

Fig. 10 and Fig. 11 show results of the decay analysis for carrot extract and tomato extract. The IRF is shown in green, the fluorescence in blue. The red curve is a fit with a triple-exponential incomplete-decay model [2, 4]. The decay parameters are shown upper right.

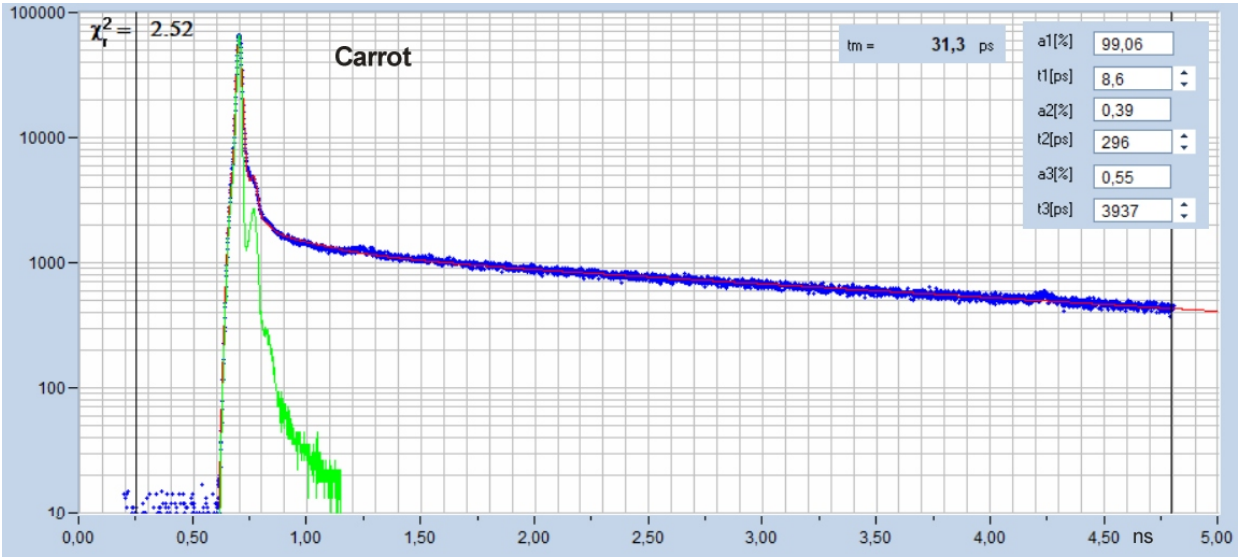


Fig. 10: SPCImage decay analysis of carrot extract. Blue: Fluorescence. Green: IRF. Red: Fit with triple-exponential model. Decay parameters shown upper right.

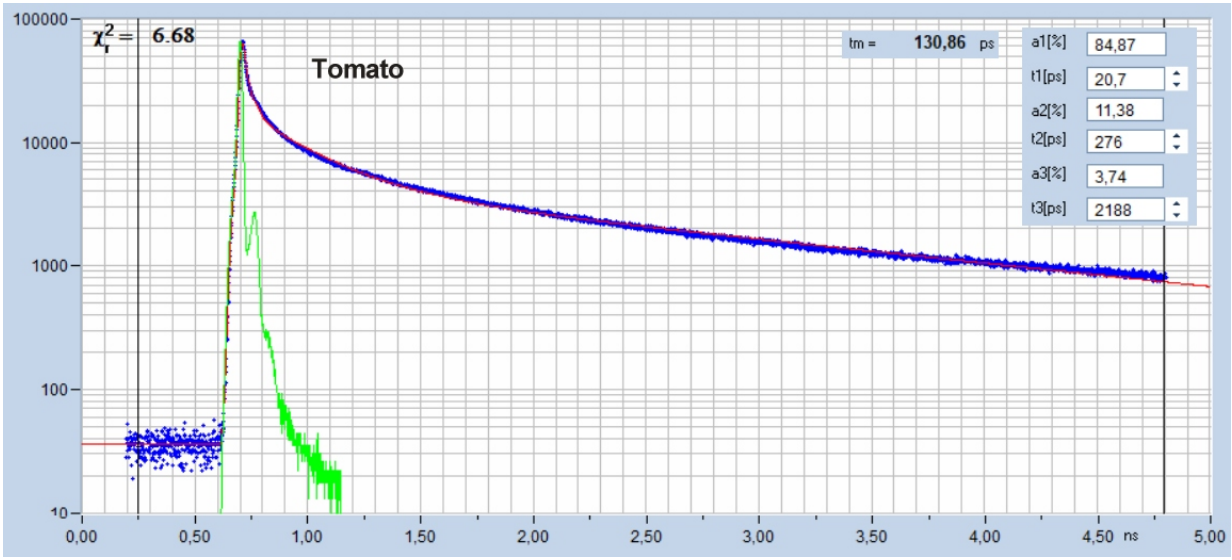


Fig. 11: SPCImage decay analysis of tomato extract. Blue: Fluorescence. Green: IRF. Red: Fit with triple-exponential model. Decay parameters shown upper right.

The decay data of the samples investigated are summarised in Fig. 12. Based on fits of different data sets and fits with different model options we estimate that the accuracy of the fast-component lifetime, t1, is about ±2 ps, if not better.

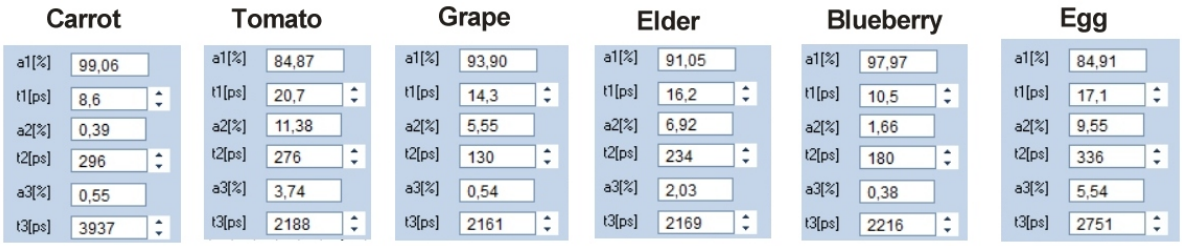


Fig. 12: Decay parameters of the samples investigated

## Summary

Using the bh DCS-120 MP multiphoton FLIM system, we were able to record fluorescence decay data of natural carotenoids and anthocyanins. Although these compounds are often considered non-fluorescent the system had no problem to record their decay functions and determine the lifetimes. In all cases, the decay was dominated by an ultra-fast decay component, with a lifetime in the range of 8.6 ps to 20 ps and an amplitude of 84% to 99%.

## References


1. W. Becker, Advanced time-correlated single-photon counting techniques. Springer, Berlin, Heidelberg, New York, 2005
2. W. Becker, The bh TCSPC handbook. 9th edition. Becker & Hickl GmbH (2021), www.becker-hickl.com, printed copies available from bh
3. Becker & Hickl GmbH, The bh TCSPC Technique. Principles and Applications. Available on www.becker-hickl.com.
4. SPCImage NG Next Generation FLIM Data Analysis Software. Overview brochure, available on www.becker-hickl.com
5. Becker & Hickl GmbH, Sub-20ps IRF Width from Hybrid Detectors and MCP-PMTs. Application note, available on www.becker-hickl.com
6. Becker & Hickl GmbH, DCS-120 Confocal and Multiphoton FLIM Systems, user handbook, 9th ed. (2021). Available on www.becker-hickl.com
7. Becker & Hickl GmbH, Two-Photon FLIM with a femtosecond fibre laser. Application note, available on www.becker-hickl.com
8. W. Becker, Lukas Braun, A. Bergmann, High-Resolution Measurement of NADH and FAD Fluorescence Decay with the DCS-120 MP. Application note (2021), available on www.becker-hickl.com
9. W. Becker, J. Breffke, B. Korzh, M. Shaw, Q-Y. Zhao, K. Berggren, 4.4 ps IRF width of TCSPC with an NbN Superconducting Nanowire Single Photon Detector. Application note, available on www.beker-hick.com
10. T. Bhatt, K. Patel, Carotenoids: Potent to prevent diseases review. Natural Products and Bioprospecting 10:109-117 (2020)
11. J. A. Fernández-López, V. Fernandez-Lledó, J. M. Angosto, New insights into red plant pigments: more than just natural colorants. RCS Adv. 20, 24669-24682 (2020)
12. T. Gillbro, R.J. Cogdell, Carotinoid Fluorescence. Chem. Phys. Lett. 158, 312-316 (1989)
13. T. Maoka, Carotenoids as natural functional pigments. Journal of Natural Medicines 74:1-16 (2020)
14. D. Niedzwiedzki, J. F. Koscielecki, H. Cong, J. O. Sullivan, G. N. Gibson, R. R. Birge, H. A. Frank, Ultrafast dynamics and excited state spectra of open-chain carotenoids at room and low temperatures. J. Phys. Chem. B 111, 5984-5998 (2007)
15. H. Scheer, Pigmente und antennenkomplexe. In: D.-P. Häder (ed.), Photosynthese. Georg Thieme Verlag, Stuttgart, New York. (1999)
16. D. Schweitzer, S. Schenke, M. Hammer, F. Schweitzer, S. Jentsch, E. Birckner, W. Becker, Towards metabolic mapping of the human retina. Micr. Res. Tech. 70, 403-409 (2007)
17. J. Yabuzaki, Carotenoids Database: structures, chemical fingerprints and distribution among organisms. Database, 2017, 1–11, doi: 10.1093/database/bax004